RESEARCH PAPER

Prediction of area burned under climatic change scenarios: A case study in the Great Xing'an Mountains boreal forest

YANG Guang • DI Xue-Ying • ZENG Tao • SHU Zhan •
WANG Chao • YU Hong-Zhou

Abstract: Monthly projections of maximum temperature, relative humidity, precipitation, and wind speed were made based on the model of HadCM3 and the climatic change scenarios of IPCC SRES A2a and B2a for the future scenario periods of 2010–2039 (referred to as 2020s), 2040–2069(referred to as 2050s), and 2070–2099(referred to as 2080s). The period 1961–1990 was chosen as the baseline period. The observed and projected weather data were downscaled using delta change methods and historical relationships between weather data, area burned, and the seasonal severity rating (SSR) code of the Canadian Fire Weather Index System were examined. The variations of area burned as influenced by climate change were assessed quantitative and qualitative for the study region, assuming that the fire regimes had the similar responses to the warming climate as during the 20th century. Our results indicated that a linear regression relationship existing between the historical area burned and the mean SSR values with regression coefficient in the significant range of 0.16 to 0.61. It was evident that the increased SSR values could result in more area burned; the area burned in the study region would have an increasing pattern during the 21st century under scenarios A2a and B2a scenarios and the area burned would be doubled. Also, the future area burned would have a strong seasonal pattern that more fires would occur in summer and autumn fire season, especially in summer. The area burned in summer fire season would increase by 1.5 times compared to that in the baseline period in 2080s under A2a scenarios.

YANG Guang • DI Xue-ying   (✉) • ZENG Tao •   SHU Zhan
WANG Chao • YU Hong-zhou
College of Forestry, Northeast Forestry University, Harbin 150040, P.R. China. E-mail: dixueying@126.com

Responsible editor: Chai Ruihai

Keywords: climatic warming; forest fire; area burned; forecast

Introduction

Fire is one of the dominant disturbances in China's boreal forest. Although China's forest cover has grown from approximately 12% to more than 20% through sustainable forest management over the past 30 years (He et al. 2007; He et al. 2008; Zhu. 2009), the forest area affected by fires increases continually at an alarmingly rate of 0.6 million hectares per year. Area burned can be strongly influenced by a complex set of variables, such as climate/weather, ignition, fuel and fire control activity, especially climate/weather (Flannigan et al. 1991; Wheaton.2001). Recently, the climate has been warming as a result of an increasing concentration of greenhouse gases and aerosols in the global atmosphere composition (Douville, 2002). The global average surface temperature has increased by 0.74ºC during the last 100 years (IPCC et al. 2007). China's temperature rise has kept the same pace with global warming (Ding et al.2006). Such warming is likely to have a significant impact on area burned. It is suggested that the observed increase in area burned of China due to climate warming, for example, the average annual area burned of the total forest area increased from 0.5% in 1990–1999 to 0.8% in the period of 2000–2009. However, this warming has not been uniform across the whole country. Most of the warming in China over the last 50 years has been in the Northern Hemisphere upper latitudes, where the Great Xing'an Mountains boreal forest resides (Fang et al. 2000; Jia et al. 2009). The most productive forests area located in the Great Xing'an Mountains in northeastern China, unfortunately, this region is always associated with high forest fire danger rating. Hence, study on the future area burned trends in the Great Xing'an Mountains is important in advancing the understanding of the climate change on forest fire regimes of boreal ecosystem.

In recent years, there are a few methods available to estimate future area burned, and the use of the 21st century climate simulations of General Circulation Models (GCMs) and the historical

<img>Springer logo</img>

relationships between observed area burned and associated weather and fire weather index seems to be an appropriate methodology to apply (Flannigan et al. 2005; Tymstra et al. 2007; Carvalho et al. 2009; Krawchuk et al.2009). For instance, Flannigan et al. (2005) estimated that area burned in Canada may increase by 74%–118% by the end of 21st century using historical relationships between weather/fire danger and area burned in tandem with two GCMs and these estimates do not explicitly take into account any changes in vegetation, ignitions, fire season length or human activity that may influence area burned. Tymstra et al. (2007) estimated the area burned based on the historical frequency of area burned using Canadian Forest Fire Weather Index (CFFWI) system class. Carvalho et al. (2008) performed regressions for the area burned and fire occurrence with the meteorological and FWI variables. Balshi et al. (2008) developed relationships between air temperature and fuel moisture codes derived from the CFFWI system to estimate annual area burned using Multivariate Adaptive Regression Spline approach across Alaska and Canada.

The objective of this study was to predict the area burned in Great Xing'an Mountains boreal forests by forest fire for the 21st century. To our knowledge, a number of the studies on future area burned as influenced by climate change are underway, however, nearly all these studies are conducted in North America, Europe and no previous studies have addressed this issue in China.

Materials and methods

Study area

The study area covers approximately 8.35 million hectares of Great Xing'an Mountains, northeastern China (50°10′–53°33′ N, 121°12′–127°00′ E). The study region comprises three counties (Mohe, Tahe, Huma) and four districts (Jiagedaqi, Songling, Xinlin, Huzhong) (Fig.1). The region has a typical continental climate, with long, cold winters and short, cool summers. The mean annual temperature is -2.8℃ and total annual precipitation is 746 mm. Elevation varies gradually from approximately 300 to 700 m. The dominant species in the region area are *Larix gmelini*, *Betula platyphylla*, *Pinus sylvestris* var. *mongolica, etc.* (Xu, 1998). It is observed that the species of higher dominance in the landscape area are more prone to wildfires.

Data collection

Forest fires data

Forest fire records were obtained from the local fire management agencies of the Great Xing'an Mountains. The fire records from 1966 to 2008 include the date of ignition, location, ignition cause, fire size. There are two fire seasons in this region: the spring fire season (15 May to 15 June) and the autumn fire season (15 September to 15 November). Forest fires occur throughout the fire seasons; however, recently they are becoming more frequent and burning large areas in summer months. Many studies have fo-

cused on forest fires in summer, and have considered the time period from 16 June to 14 September as the summer fire season (Zhang 2008; Zhang 2009; Zhang et al. 2010). In this paper, all fire records during the three fire seasons were included in the analysis for consistency with the meteorological records.
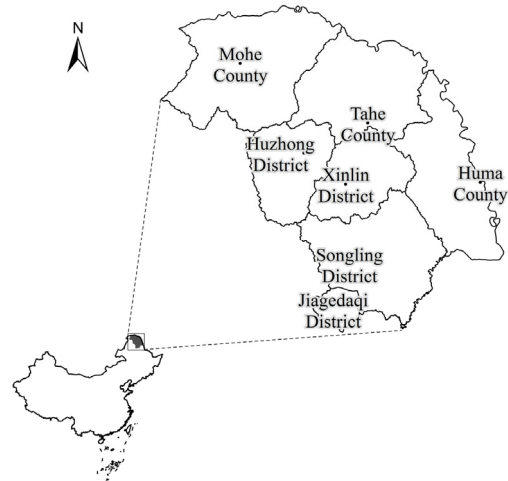

Fig. 1 Location and administrative division of Great Xing'an Mountains, northeastern China.

Meteorological data

The meteorological data for the study were obtained from China Meteorological Data Sharing Service System (http://cdc.cma.gov.cn/) for the same period as the fire data from 1966 through 2008. Eighteen meteorological stations were selected for analysis (see Table 1). For each station, the data contained daily maximum temperatures, 24–h precipitation, mean wind speed, and mean relative humidity. Not all the stations have equally complete meteorological records (Table 1). To fill these gaps, the stations with intermittent meteorological data were estimated by linear regression from the nearest stations.

Climatic scenarios

The climate change simulations produced by the third version of the UK Meteorological Office's Hadley Centre Coupled Model (HadCM3) were used to estimate the discharge of the study area. HadCM3 is the tool most commonly used to project future climate and exhibits better performance in East Asia. The model requires no artificial flux adjustments to prevent excessive climate drift and its dynamics and physics are solved on a 3.75°×2.5° longitude–latitude model grid with 19 hybrid vertical levels (Carson 1999 and Lynch 2008). The climate change scenarios were obtained from the Intergovernmental Panel on Climate Change (IPCC) Data Distribution Centre (http://www.ipcc-data.org/). Within the IPCC Special Report on Emission Scenarios (SRES), the SRES A2a and B2a scenarios were used in this analysis. Both A2a and B2a describe a "regionalization", meaning a heterogeneous world development. A2a describe a highly heterogeneous future world with regionally oriented economies. The B2a is also regionally oriented but with a general evolution towards environmental protection and social equity. Compared to A2a, B2a has a lower rate of population

growth, a smaller increase in GDP but more diverse technological changes and slower land-use changes (Nakicenovic et al. 2000; Leckebusch et al. 2004). The variables available for HadCM3 were expressed as 30-year monthly mean values, calculated for the baseline period 1961–1990 (refers to here as 1980s), and predicted fields for the 2010–2039 (refer to as 2020s), 2040–2069 (refer to as 2050s), and 2070–2099 (refers to as 2080s) (Arnell 2003). The climatic variables available for the two scenarios include mean maximum temperature, mean precipitation, wind speed and relative humidity.

Table 1. The information of meteorological stations used in the statistical analyses

Station name	Latitude	Longitude	Elevation(m)	Start year	Missing Year
Mohe	52.97	122.52	433.0	1957	1958
Tahe	52.35	124.72	361.9	1960	1962-1971
Xinlin	51.70	124.33	494.6	1972	——
Huma	51.72	126.65	177.4	1954	——
Amuer	52.83	123.18	550.0	1974	——
Huzhong	52.05	123.67	520.8	1974	——
Eergunayouqi	50.25	120.18	581.4	1957	——
Tulihe	50.48	121.68	732.6	1957	——
Daxinganling	50.40	124.12	371.7	1966	——
Heihe	50.25	127.45	166.4	1959	——
Xiaoergou	49.20	123.72	286.1	1957	——
Nenjiang	49.17	125.23	242.2	1951	——
Sunwu	49.43	127.35	234.5	1954	——
Boketu	48.77	121.92	739.7	1951	——
Zhalantun	48.00	122.73	306.5	1952	——
Beian	48.28	126.52	269.7	1958	——
Keshan	48.05	125.88	234.6	1951	——
Fuyu	47.80	124.48	162.7	1956	——

Statistical analyses

Delta change methods
Daily rather than monthly data were used because the weather and, consequently, fire behavior can change dramatically over time periods much shorter than a month. Downscaling methods were thus needed to bridge the gap between the large scale climate scenarios and the finer local climate scale and to change monthly climate variability into daily local climate variability. Delta change approach was used in this paper, which is very simple and has been used in many climate change impact studies (Lenderink et al. 2007; Zhao FF et al. 2007; Akhtar et al. 2008). The monthly climatic variables (temperature, humidity, precipitation and wind speed), obtained for the period 1980s and predicted mean monthly change fields for 2020s, 2050s, and 2080s for both A2a and B2a simulations, were downscaled by delta change approach for the regional model simulations. The four daily climatic variables for the future time series between the two simulations were computed according to the following equations:

$$T_{f,daily} = T_{o,daily} + \left(\overline{T_{f,monthly}} - \overline{T_{p,monthly}} \right) \tag{1}$$

$$P_{f,daily} = P_{o,daily} \frac{\overline{P_{f,monthly}}}{\overline{P_{p,monthly}}} \tag{2}$$

$$R_{f,daily} = R_{o,daily} \frac{\overline{R_{f,monthly}}}{\overline{R_{p,monthly}}} \tag{3}$$

$$W_{f,daily} = W_{o,daily} \frac{\overline{W_{f,monthly}}}{\overline{W_{p,monthly}}} \tag{4}$$

Where, $T_{f,daily}$, $P_{f,daily}$, $R_{f,daily}$ and $W_{f,daily}$ are the future daily temperature (ºC), precipitation(mm), relative humidity (%) and wind speed (m/s); $T_{o,daily}$, $P_{o,daily}$, $R_{o,daily}$ and $W_{o,daily}$ are the daily observations; $\overline{T_{f,monthly}}$, $\overline{P_{f,monthly}}$, $\overline{R_{f,monthly}}$ and $\overline{W_{f,monthly}}$ are the mean monthly HadCM3 simulated future temperature(ºC), precipitation(mm), relative humidity(%) and wind speed(m/s); $\overline{T_{p,monthly}}$, $\overline{P_{p,monthly}}$, $\overline{R_{p,monthly}}$ and $\overline{W_{p,monthly}}$ are the mean monthly HadCM3 simulated present temperature(ºC), precipitation(mm), relative humidity (%) and wind speed (m/s).

Forest fire weather index
The CFFWI system consists of six components: three fuel moisture codes (Fine Fuel Moisture code, Duff Moisture Code, Drought Code) and three fire behaviour indices (Initial Spread Index, Build Up Index, Fire Weather Index). The Fire Weather Index (FWI), a daily measure of potential fire danger, is derived from daily temperature, relative humidity, wind speed, and 24-h precipitation. The FWI is used to predict the intensity of a spreading fire, largely by estimating the state of forest fuels. The FWI is also used to estimate the fire hazard warning that is commonly posted in the Canadian northern communities. The Daily Severity Rating (DSR) is calculated from the FWI according to the following equation:

$$DSR = 0.0272(FWI)^{1.77} \tag{5}$$

The purpose of the DSR is to weigh the FWI to improve estimates of the effort required to control a fire under different conditions. By averaging DSRs over a period, one can obtain the Seasonal Severity Rating (SSR). The SSR, a final component of CFFWI system (Van Wagner C E, 1987), was used to measure fire seasonal variation within the climate of the region in this study. The SSR was calculated as the mean seasonal Daily Severity Rating of all meteorological stations in the region over the fire season.

Results and discussion

Area burned trends

Historically fire has a strong impact on the vegetation in Great Xing'an Mountains. Current estimates indicated that an average

of 0.15 M ha was burned annually across the entire study region since 1966. Fires in 1966, 1972, 1977, 1987 and 2003 caused enormous damage to the area burned (more than 0.7 M ha). Although there is great year-to-year variability of average annual area burned, there is evidence that the area burned has decreased dramatically in recent decades as a result of strict enforcement of the fire suppression policy. The average area burned has decreased more than 80% since 1990. Analysis of average areas burned by decades revealed a bimodal distribution with distinct low and extreme high area burned years (see Fig.1). Statistical evidence suggested that there has been a decreasing trend in area burned starting in the early 1980–1989 period and continuing into the 1990–1999 period. The projected fire statistics showed an increase pattern from 2000 and onwards.
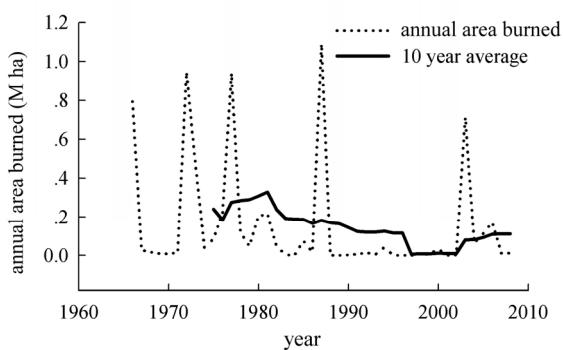

Fig. 1 Annual mean area burned in the period of 1966-2008 for Great Xing'an Mountains.

Based on the fire information provided, area burned in the study region is strongly seasonal, with 83.9% of area burned occurred in the spring fire season during 1966–2008. Also in the same period, a significant increase of area burned happened in the summer time. Since 2000, wildfires have burned approximately 35 520 ha in the summer fire season around this region, which are accounted for 36.7% of that since 1966. The monthly time span of area burned ranged from the beginning of March to the end of October (see Fig.2). On average, May is the month with the highest area burned.
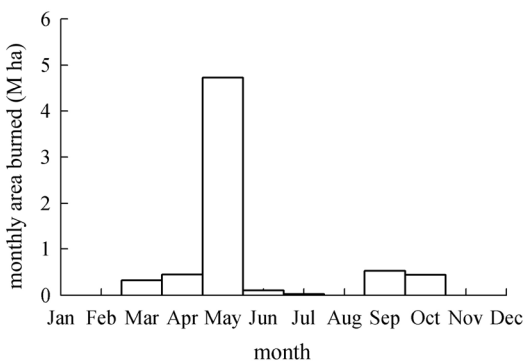

Fig. 2 Monthly mean area burned in the period of 1966-2008 for Great Xing'an Mountains.

Relationship between forest fires and fire weather indices

To examine the relationship between area burned and the mean seasonal SSR value for the period 1961–1990, Linear regression analyses were conducted between area burned and the SSR values with the latter as independent variable for the four fire seasons (Fig. 3: a is the whole fire season, b is the spring fire season, c is the summer fire season, d is the autumn fire season). It is found that good linear relationships exist between the two variables for the four fire seasons with regression coefficients ranging from 0.16 to 0.61. It is interesting to note the linear relationship between area burned and the SSR value for the autumn fire season is the strongest among the four fire seasons, with the regression coefficient 0.61 as the highest.
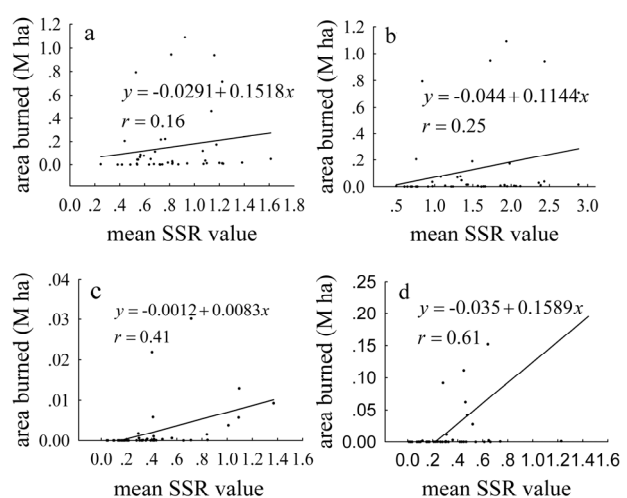

Fig. 3 The relationship between area burned and mean SSR values during 1961–1990 period (a: the whole fire season; b: spring fire season); c: summer fire season; d: autumn fire season)**.

Time series of SSR over the Chinese boreal forest

SSR was calculated for all eighteen meteorological stations, and these SSRs were interpolated to generate a SSR grid to cover the study region. Fig. 4 includes such interpolated grids for the mean 30-year SSR values under both A2a and B2a scenarios, respectively. The SSR values ranged from 0.01–1.20 across the study region, and obviously SSR values showed an increasing pattern in the future compared to the baseline period. The fastest increase in the mean 30–year SSR happens in the summer fire season, and the second fastest increase is in the autumn fire season.

Conclusion

In this study, we estimated the area burned in China's boreal forest for the 21st century. Our results indicate that area burned would increase in the study region with continuing global

warming, and the results are similar to those found in previous studies conducted in Canada, USA, Russia, and Portugal. A significant relationship was found between historical area burned and the mean SSR values in the study region, which can be illustrated by a simple linear regression with regression coefficient ranging from 0.16 to 0.61. Considerable evidences suggest that the increasing SSR value could translate into increasing area burned, and this finding is in accordance with that as found in Canada's boreal forest using two GCMs (Flannigan et al. 2005). According to the Hadcm3 model, the area burned would increase from 20% to 174 % across the most study region for the period 2010–2099 under both scenarios of A2a and B2a. Furthermore, area burned would peak in 2080s under both scenarios, and area

burned would increase by 20–174% under the A2a scenario and by 25–105% under the B2a scenario. The study region would experience 20–85% increase in area burned in the spring fire season under the A2a scenario, and 27–65% under the B2a scenario. However, the highest increase in area burned would appear in the summer fire season. The study region may experience an increase in area burned of 174% under A2a scenario and 106% under B2a scenario for 2080s. Alternatively, the region would face an increase of 22–174% in area burned in the spring fire season under the A2a scenario, and an increase of 25–106% under the B2a scenario. The results provided in this study may provide important information on how area burned is influenced by climatic changes for the fire management in the study region.
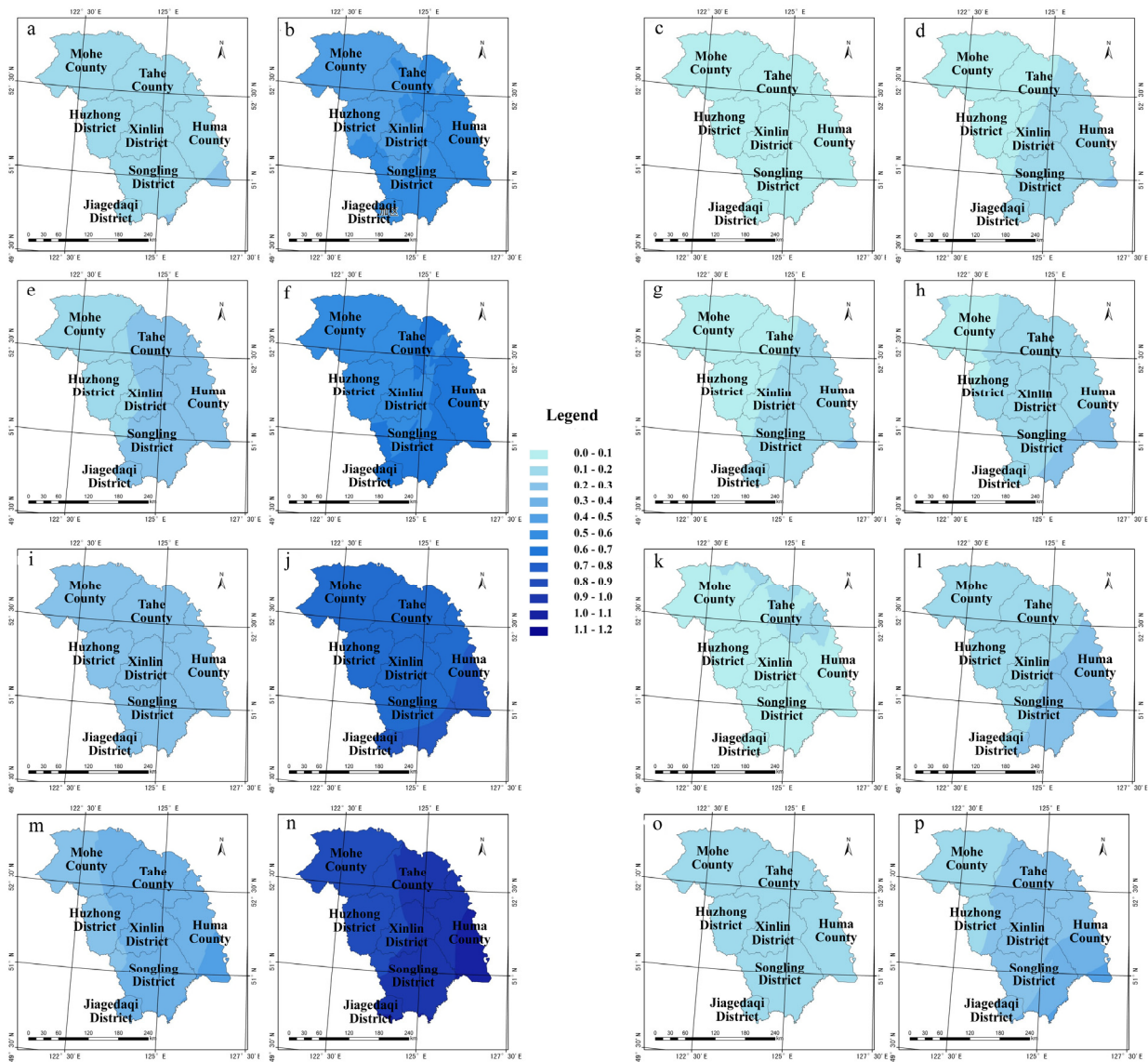

Fig. 4 Seasonal mean SSR (SMS) values for the baseline and the three future under A2a scenarios (a: the whole SMS for the baseline period; b: spring SMS for the baseline period; c: summer SMS for the baseline period; d: autumn SMS for the baseline period; e: the whole SMS for 2020s; f: spring SMS for 2020s; g: summer SMS for the 2020s; h: autumn SMS for the 2020s; i: the whole SMS for 2050s; j: spring SMS for 2050s; k: summer SMS for the 2050s; l: autumn SMS for the 2050s; m: the whole SMS for 2080s; n: spring SMS for 2080s; o: summer SMS for the 2080s; p: autumn SMS for the 2080s).

References

Akhtar M, Ahmad N, Booij MJ. 2008. The impact of climate change on the water resources of Hindukush–Karakorum–Himalaya region under different glacier coverage scenarios. *Journal of Hydrology*, **335**: 148–163.

Arnell NW.2003. Effects of IPCC SRES emissions scenarios on river runoff: a global perspective. *Hydrology and Earth System Sciences*, **7**(5): 619–641.

Balshi MS, McGuire AD, Duffy P, Flannigan MD, Walsh JE, Kicklighter DW, Melillo J. 2008. Assessing the response of area burned to changing climate in western boreal North America using Multivariate Adaptive Regression splines (MARS) approach. *Global Change Biology*, 15(3): 578–600.

Carson DJ.1999.Climate modeling: Achievements and prospects. *Quarterly Journal of the Royal Metrological Society*, **125**: 1–27.

Carvalho A, Flannigan MD, Logan KA, Gowman LM, Miranda AI, Borrego C. 2009. The impact of spatial resolution on area burned and fire occurrence projections in Portugal under climate change. *Climatic Change*, **98**: 177–197.

Carvalho A, Flannigan MD, Logan K, Miranda AI, Borrego C. 2008. Fire activity in Portugal and its relationship to weather and the Canadian Fire Weather Index System. *International Journal of Wildland Fire*, **17**: 328–338.

Ding Yihui, Ren Guoyu, Shi Guangyu, Gong Peng, Zheng Xunhua, Zhai Panmao, Zhang Deer, Zhao Zongci, Wang Shaowu, Wang Huijun, Luo Yong, Chen Deliang, Gao Xuejie, Dai Xiaosu. 2006. National assessment report of climate change (I): Climate change in China and its future trend. *Advances in Climate Change Research*, **2**(1): 3–8. (in Chinese)

Douville H, Chauvin F, Planton S, Royer JF, Salas-Melia D, Tyteca S. 2002. Sensitivity of the hydrological cycle to increasing amounts of greenhouse gases and aerosols. *Climate Dynamics*, **20**: 45–68.

Fang Jingyun, Tang Yanhong, Lin Junda, Ge Gaoming et al. 2000.*Global ecology: Climate change and ecological responses*. Beijing: Higher Education Press, Springer Press, p189. (in Chinese)

Flannigan MD, Amiro BD, Logan KA, Stocks BJ, Wotton BM.2005. Forest fires and climate change in the 21st century. *Mitigation and Adaptation Strategies for Global Change*, **11**: 847–859.

Flannigan M D, Logan K A, Amiro B D, Skinner W R, Stocks B J.2005. Future area burned in Canada. *Climatic Change*, **72**: 1–16.

Flannigan MD, Stocks BJ, Wotton BM.2000. Forest fires and climate change. *Science of the Total Environment*, **262**: 221–230.

Flannigan MD, Van Wagner CE.1991.Climate change and wildfire in Canada. *Canaian.Journal of Forest Reearch,* **21**(1): 66–72.

He Fanneng, Ge Quansheng, Dai Junhu, Lin Shanshan. 2007.Quantitative analysis on forest dynamics of China in recent 300 years. *Acta Geographica Sinica*, **62**(1): 30–40. (in Chinese)

He FN, Ge QS, Dai JH, Rao YJ. 2008. Forest change of China in recent 300 years. *Journal of Geographical Sciences*, **18**(1): 59–72.

IPCC.2007.Climate Change 2007: The physical science basis Intergovernmental Panel on Climate Change. Http://www.ipcc.ch/.

Jia Bingrui, Zhou Guangsheng. 2009. Advance in the studies of response of boreal foreset to climate change. *Advances in Earth Science*, **24**(6): 668–674. (in Chinese)

Krawchuk MA , Cumming SG, Flannigan MD. 2009. Predicted changes in fire weather suggest increases in lightning fire initiation and future area burned in the mixedwood boreal forest. *Climatic change*, **92**: 83–97.

Lenderink G, Buishand A, Deursen WV. 2007. Estimates of future discharges of the river Rhine using two scenario methodologies: Direct versus delta approach. *Hydrology and Earth System Sciences*, **11**(3): 1145–1160.

Leckebusch GC, Ulbrich U.2004. On the relationship between cyclones and extreme windstorm events over Europe under climate change. *Global and Planetary Change*, **44**: 181–193.

Lynch P.2008.The origins of computer weather prediction and climate modeling. *Journal of Computational Physics*, **227**(7): 3431–3444.

Nakicenovic N, Alcamo J, Davis G, De VB, Fenhann J, Gaffin S, Gregory K, Grubler A, Jung TY, Kram T, La R et al. 2000. *Special report on emissions scenarios: A special report of Working Group III of the Intergovernmental Panel on Climate Change*. New York: Cambridge University Press, p4–5.

Tymstra C, Flannigan MD, Armitage OB, Logan K. 2007. Impact of climate change on area burned in Alberta's boreal forest. *International Journal of Wildland Fire*, **16**(2): 153–160.

Van Wagner CE. 1987. *Development and structure of the Canadian forest fire weather index system*. Ottawa: Canadian Forestry Service, p1–7.

Wheaton E.2001.*Changing fire risk in a changing climate: a literature review and assessment*. Saskatchewan: Saskatchewan Research Council Publications, p8–9.

Xu Huacheng. 1998. *Great Xing' an Mountains forest*. Beijing: Science Press, p1–8 (in Chinese)

Zhang Huilian. 2009. Preliminary study on reasons for summer forest fire and its characteristics in Daxinganling area. *Forest Inventory and Planning*, **34**(5): 54–56. (in Chinese)

Zhang Siyu, Li Jie. 2010. Temporal and spatial distribution rule of summer forest fire in China. *Journal of Anhui Agriculture*, **38**(3): 1551–1553. (in Chinese)

Zhang Siyu. 2008. Current situation and tendency of summer forest fires. *Journal of Institute of Disaster-Prevention Science and Technology*, **10**(3):1–5. (in Chinese)

Zhao Fangfang, Xu Zongxue. 2007. Comparative analysis on downscaled climate scenarios for headwater catchment of yellow river using SDS and delta methods. *Acta Meteorologica Sinica*, **65**(4): 653–661. (in Chinese)

Zhu Yong. 2009. The seventh national forest resources inventory .*Land Greening*, (12):5–7. (in Chinese)

Springer

波[1], 刘斌[1](1. 华南农业大学林学院, 广东 广州 510642; 2. 琉球大学理学部, 日本冲绳 903-0213, 日本) // Journal of Forestry Research. –2010(2). 207~212

2008 年 1 月至 2 月, 我国南方发生了严重的冰雪灾害, 受害的森林地面积达 2.09×10^{6} km[2]。为了了解冰雪灾害对杉木的损害和由此引起的林地养分分布特点, 作者调查粤北一个杉木林地的受害情况。冻雨在杉木枝叶上形成冰柱, 造成所有的林木折冠。林木折断的高度和胸径呈显著相关。树冠残体的养分总浓度随残体组分而变化, 呈现叶>皮>枝>干。树冠残体的干重达 19.11t·hm[-2], 枝、树干、叶和皮分别占 37%、28%、27%和 8%。2008 年树冠残体的养分分布随组分而急剧变化, 其中叶的养分量占残体养分总量的 70%, 枝、干和皮分别占 13%、7%和 10%。2008 年杉木林地的 N、P、K 的积累量为 105067.9 t·hm[-2], 杉木残体、凋落物和土壤分别占 0.18%、0.03% 和 99.79%。养分积累量在树冠残体各组分和凋落物中的排序为 N>K>P, 而在土壤中为 K>N>P。2009 年的凋落物中 N 和 P 浓度大于 2008 年的凋落物, 而 K 浓度小于后者。2009 年的干和皮残体中 N 和 P 浓度略大于 2008 年的干和皮残体, 而 K 浓度正好相反。2009 年的干和皮残体中的 N 和 P 储量与 2008 年接近, K 储量略小于后者。2009 年的凋落物中 N、P 和 K 储量大于 2008 年的凋落物。图 1 表 5 参 38。

关键词: 树冠残体; 杉木; 冰雪灾害; 凋落物; 养分; 土壤

2010-02-16

气候变化下森林火灾过火面积预测---以大兴安岭北方森林为例=Prediction of area burned under climatic change scenarios: A case study in the Great Xing'an Mountains boreal forest[刊, 英]/杨光, 邸雪颖, 曾涛, 舒展, 王超, 于宏洲(东北林业大学, 哈尔滨 150040) // Journal of Forestry Research. –2010(2): 213~218

利用Delta统计降尺度方法解集HadCM3 IPCC SRES A2a 和B2a情景下气候基准时段（1961–1990年）与未来不同时段（21世纪20年代, 2010–2039年; 21世纪50年代, 2040–2069 年; 21世纪80年代, 2070–2099年）的逐月的最高温度、相对湿度、降水和风速数据, 结合历史火灾数据、气象资料以及加拿大火险天气指标系统中SSR指标数值的统计相关性, 在假设林火动态对当前及未来气候变化具有相同响应方式的基础上, 定量和定性相结合预估未来该区北方森林过火面积的变化趋势。结果表明: 历史过火面积与SSR均值呈显著线性相关（r, 0.16–0.61）, SSR增值能作为过火面积增量指标。HadCM3 IPCC SRES A2a和B2a情景下, 21世纪大兴安岭地区森林火灾过火面积相对于1961–1990年气候基准值呈显著增加趋势, 其中21世纪80年代该区平均过火面积可能会增加1倍。21世纪该区过火面积呈现强烈的季节特征, 夏季防火期和秋季防火期的过火面积增长较快, 尤其是夏季防火期, A2a 情景下21世纪80年代森林火灾过火面积将会增加1.5倍。图4 表1参31。

关键词: 气候变暖; 林火; 过火面积; 预测

2010-02-17

稻壳-聚乙烯复合材料经历自然老化后的性能变化= Performance of rice-hull-PE composite exposed to natural weathering[刊, 英]/王伟宏, 卜凡华, 张征明, 隋淑娟, 王清文(东北林业大学, 生物质材料科学与技术教育部重点实验室, 哈尔滨 150040, 中国) // Journal of Forestry Research. –2010(2). 219~224

稻壳粉被广泛地应用于聚合物复合材料, 但对这些复合材料的耐老化性能研究得还很少。本文研究了两种稻壳粉/聚乙烯(RH-PE)复合板经过两年室外自然老化以后的性能变化。试件的抗弯强度和弹性模量没有变化。但在试验结束后试件的亮度增加了 23%以上, 总色差变化 9 个单位以上, 意味着消费者当初挑选的颜色发生了明显变化。傅立叶红外（FTIR）和 X 射线光电子能谱(XPS)分析显示, 试件表面发生了氧化反应, 老化后红色板材产生明显的 C=O 峰, 但黄色板材的 C=O 峰并没有明显变化。两种板材都显示木素纤维素减少和聚乙烯的无定形区域减少。图 7 表 4 参 16。

关键词: 稻壳; 聚乙烯; 复合材; 老化

2010-02-18

尼加拉瓜西南部热带雨林生态系统木材生产速率及其对可持续森林经营的启示=Rate of timber production in a tropical rainforest ecosystem of Southwestern Nigeria and its implications on sustainable forest management[刊, 英]/ V. A. J. Adekunle[1], A. O. Olagoke[1], L. F. Ogundare[2] (1. Federal University of Technology, Department of Forestry and Wood Technology, Akure, Nigeria; 2. Ondo State Ministry of Agriculture, Forestry and Fisheries, Forestry and Wildlife Services, Akure, Nigeria) // Journal of Forestry Research. –2010(2). 225~230

积累木材采运数据对森林可持续经营是非常必要的, 但这些数据在一些发展中国家却非常缺乏。本文收集和分析了尼加拉瓜 Ondo 州森林保护区和非保护区内木材生产速率的数据。数据来源于州林业主管部门的官方数据、年度报告和相关文件, 包括 2003 年至 2005 年间以月采伐量为单位的不同经济木材的物种、材积量和立木数。对收集的数据进行 T 检验和一维方差分析。结果表明: 3 年间, 非保护区内采伐木材的物种数、科数和立木量均高于森林保护区内采伐的。但是, 保护区内被砍伐的树木材积总量要显著高于非保护区的($p<0.05$)。非保护区内, 有 25 个植物科的 60 种阔叶树种被砍伐; 森林保护区内有 23 个科的 57 种阔叶树种被砍伐。3 年间, Ondo 州森林系统内被砍伐树木共 111,377 株, 材积量约 295 089.67 m[3]。年平均伐木数和材积量分别是 37,125 株和 98 363.22 m[3]。月平均伐木数和材积量分别是 3 094 和 8 196 m[3]。T 检验结果表明, 森林保护区和非保护区内被砍伐的树木株数和材积量显著不同($p<0.05$)。一维方差分析结果表明,